International Journal Of Electronics Engineering (Issn: 0973-7383)
Volume 10 • Issue 2 pp. 201-209 June 2018-Dec 2018 www.csjournals.com

Multi-focus Image Fusion using Modified Gaussian filter and Discrete Lifting Wavelet Transform

Tarlok Singh[1], Prof. Pammy Manchanda[2]
[1, 2]Guru Nanak Dev University, Amritsar, Punjab, India, 143001.
tarlok.maths@gmail.com

Abstract: Image fusion has always been a popular research area towards improving the visual quality of digital pictures. Selective picking of best parts from each image and integrating them into one work of art is called image fusion. We proposed a multi-focus image fusion method where partially blurred images are merged together and yield a better-quality image. This is done by applying fusion rules on obtained transformed images using discrete Lifting wavelet Transform (LWT). Proposed technique provides an agile ability for image fusion compared to the existing fusion techniques. The proposed algorithm is very simple to implement and faster than conventional techniques. Testing is done on a collection of standard images, with and without employing consistency verification. **Keywords: Image fusion, Digital image processing, Lifting wavelet transform, Fusion rules, Visual sensor networks.**

I. Introduction

Image fusion is the technique to blend more images while obtaining maximum information from the image and avoid noise or any fictional data [1]. The goal is to get one processed image of best quality compared to each individual input image. There are different categories of fusion such as Multi-focus, multi-sensor, single sensor, multi-view, multi-modal and multi-temporal [2].

In multi-focus image fusion method, multiple images of a given scene are obtained with focus on different objects. They are fused in such a way that most objects become concentrated in the resultant image [3]. Line Spread Function (LSF) is computed for every pixel of input images, and a segmentation of the average image is presented to dissect the original images [4]. From segmented image, a distributed region illustration is acquired to label the original images [5]. A new statistical sharpness evaluation is discussed by exploiting the spread of Wavelet Coefficients' distribution to calculate image’s blurriness [6].

Another proficient technique for fusion of digital images is used by applying variance (according to Discrete cosine transform (DCT) values). In digital image fusion the concentrated region is more informative [7]. With Visual sensor network (VSN) we are capable of increasing the focus levels using multiple cameras [8]. The pixel level image fusion is direct fusion at initial information layer. Therefore, the quantity of data kept is utmost [9]. Pixel based fusion is to create a color image same as that of natural image by altering the relationship qualities with user's aid and a number of extra changes are required [10].

A Principle component analysis (PCA) based adaptive digital image fusion method blended multi-focus images with exactly same visible direction but various focuses. Key of this approach is to explain a new strategy for evaluating each pixel's covariance matrix with the average covariance matrix [11]. To further enhance the fusion outcome, a linear PCA based local mapping can be used to produce a "new source" image of the image fusion. Then use multi-resolution decompositions to signify the input images at various scales. It has provided a multiresolution/multimodal segmentation to partition image domain at these scales [12].

Wavelet transform and fuzzy logic-based fusion outperforms modern-day cutting-edge techniques. After employing wavelet transform to input images, we compute the weight of each input image's coefficients through fuzzy reasoning. Next, fuse the coefficients through measured averaging with computed weights and get a fused image [13].

We proposed a multi-focus image fusion method where partially blurred images are merged together and yield a better-quality image. A novel Lifting wavelet transform (LWT) based image fusion technique is proposed. Gaussian filter is also modified to improve the spatial and spectral information of images.The comparison of the proposed technique is also drawn with competitive image fusion techniques by considering the visual and quantitative analysis.

The paper is organized as follow. Section 2 gives a historical background and review of literature. Section 3 explains the proposed technique. Section 4 describes performance metrics. In Section 5, we have demonstrated experimental results and comparisons with conventional algorithms to quantify that proposed mechanism outperforms other fusion techniques. Finally, the research inferences and future directions are discussed under concluding Section 6.

II. Related work

Relating with their characteristic features, image fusion methods are categorized into four types: color space, statistical/numerical, multi-resolution decomposition and radiometric/spectral algorithms [14]. DCT based digital image fusion with contrast measure depends upon a contrast evaluate. This can be determined for each 63 Alternating Components (AC coefficients) of the blocks from input images [15]. DCT based digital image fusion mode is more effective and time efficient for real-time systems by means of DCT based criteria of video or a still image [16]. The source images are split into blocks of size 8 * 8 and then DCT coefficients for each block are computed. Afterwards, fusion rule is employed wherever in the transformed block there is an increase in quantity of larger valued AC coefficients being absorbed into the merged image [17].

Multi-resolution DCT based technique for instantaneous image noise removal and fusion, showing its efficiency regarding DWT and DTCWT is given in [18]. Wavelet transforms (WT) of the source images are suitably combined, and new image is obtained by taking inverse wavelet transform (IWT) of the fused wavelet coefficients [19]. Eventually, the fused image is reconstructed by applying inverse Curvelet transform [20]. At first, the breakdown of same scene input images using Biorthogonal wavelet transform (BWT) is completed and then coefficients obtained are pooled using absolute highest selection fusion rule. Consequently, wavelet and scaling functions are applied in BWT for breakdown of source images [21]. Pending images are broken down utilizing the wavelet lifting system into four sub-bands: LL, LH, HL, HH. Then LH, HL, HH, are synthesized to acquire three directions of high-frequency information on the images [22].

Principal component analysis (PCA) based digital image fusion is a prominent system for feature detection and measurement decrease [23]. Advantage of PCA is to significantly decrease the computational needs and resulting in high acceptance to noise in experimental data [24]. It does not merely keep spectral data of the input multi-spectral image perfectly, but also improves spatial feature data of fused image to the highest degree [25]. A new digital image fusion based on locally gathered gradient and PCA transform is presented. Image fusion method starts by using the wavelet transform of input images. Afterwards, the merged local detailed coefficients are selected based on locally gathered gradient concept. Merged estimated coefficients are obtained by selection or averaging rule based upon PCA [26].

The DCT based technique is quite time efficient and straightforward when we need to save or transmit the fused image in JPG configuration [27]. Contemporary DCT domain approaches undergo a few adverse effects such as hazing or overcrowding objects that may moderate the output image's quality [28]. Denoising based upon wavelet and weight maps based upon guided filter are capable to enhance the fusion involving noise [29]. Wavelet transform can extract the spectral knowledge along with global spatial facts from initial pair of images. Sparse depiction can pull out local constituents of the images successfully [30].

Sparse feature matrix breakdown and structural straining can generate supplementary edifying image and yield superior outcomes particularly after images hold additional features [31]. For image fusion, spectral residual fetches distinctive and prominent image fusion features in frequency realm [32]. There is an image fusion technique for medical engineering based on Contourlet Transform and multi-level fuzzy reasoning strategy. Supportive data from two spatial source medical images are built into a new image which can be utilized to create medical analysis and therapy with additional accuracy [33].

III. Proposed technique

This section describes the proposed image fusion technique based upon the discrete Lifting Wavelet Ttransform.

A. Discrete LWT transform

Multiple images having dimensioin $N \times N$ are sparse using the Lifting wavelet transform . In wavelet domain, Lifting wavelet transform decomposes the images with an integer distribution. In it, small coefficients are treated as 0 to achieve a significant reconstruction outcome. LWT has much smaller data loss when applied in image fusion process.

Lifting technique is a method to implement a DWT. Complex multiplier and accumulator units are utilized to achieve LWT. It composes three steps: Split, Predict and Update. The Figure 1 depict the working of Lifting Wavelet Transform. Here, $X[n]$ represents the input pixel values. S, P and U show the split, predict and update operations, respectively. It results in two output values such as high pass and low pass output signals.

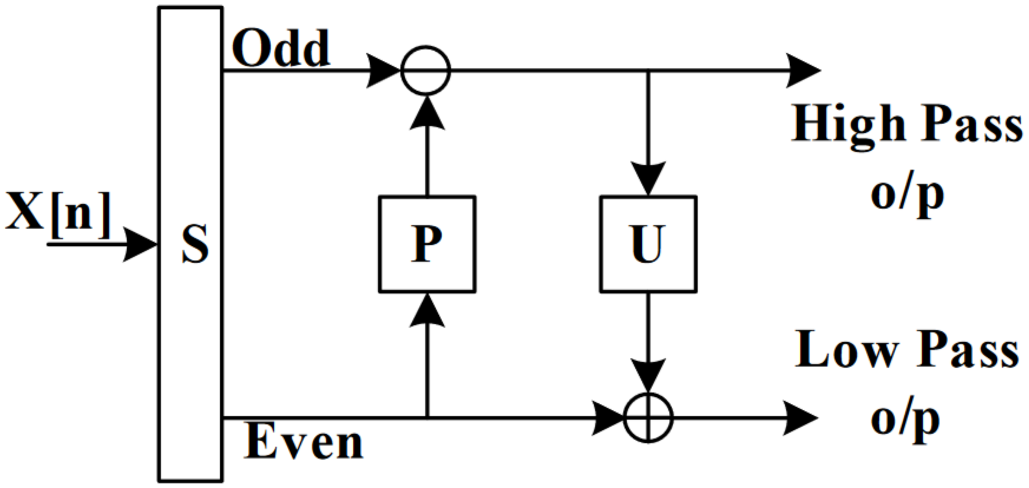

Fig. 1 Lifting scheme for DWT.

a. Split

Initially, the image is decomposed into odd (γ[i]) and even (λ[i]) segments.

$$f[k] = \begin{cases} \lambda[\mathrm{i}] = f[2k] \\ \gamma[\mathrm{i}] = f[2k+1] \end{cases} \qquad (1)$$

b. Predict

The predict operation (i.e., dual lifting) utilizes a mapping that approximates the odd segments. It provides an approximation on even segments. The odd segments of the data are replace by the difference between the approximation and the actual values. Therefore, this segment contains high pass filtered values. We can predict odd values from the even values as follows:

$$\gamma[\mathrm{i}] = \gamma[\mathrm{i}] - P(\lambda[\mathrm{i}]) \qquad (2)$$

c. Update

The update operation (i.e., primal lifting) scale and smooth the data, thereafter merged with even segments to contain low pass filtered values for DWT. It provides smoother input for the next operation of the DWT as follows:

$$\lambda[\mathrm{i}] = \lambda[\mathrm{i}] - P(\gamma[\mathrm{i}]) \qquad (3)$$

B. Modified Gaussian filter

By group of software of Gaussian filtration in an repetitive manner, the result with equally edge recovery and small structure recognition is produced. In this method a graphic I is iteratively updated. Let G be the result of the Gaussian filtration and I may be the input image. Let a and n denotes the coordinates of the pixel in the picture and σ_s, the standard deviation. The result of the Gaussian filtration may be provided with as:

$$g(x) = \frac{1}{K_x} \sum_{y \in n^o(x)} \exp\left(\frac{||-x-y^2||}{2\sigma_s^2}\right) I_{mg}(y) \qquad (5)$$

to $\sum_{y \in n^o(x)} \exp\left(\frac{||-x-y^2||}{2\sigma_s^2}\right)$ becomes the neighbourhood of a and n belongs to N(a).

The small structure are fully removed in the first step whose scale is less than σ_s^2 and the result obtained is denoted as M^{qth} iteration. The result M^{q+1th} time is received in a shared bilateral selection wherever input may be the result of the M^{qth} iteration.

$$M^{q+1} = \frac{1}{K_x}\sum_{y\in n^o(x)} \exp\left(\frac{||-x-y^2||}{2\sigma_s^2}\right)\frac{||M^q(x)-M^q(y)^2||}{2\sigma_s^2}\, I_{mg}(y) \qquad (6)$$

The repetitive strategy converges fastly to a significant picture faithful to the input picture regardless of how many repetitions have now been done.

C. Fusion process

The input source mask images are prepared with discrete LWT type-1 transform at 87,000 coefficient values. Though at this value the transform shows the side data and enhances the image globally but it escalates the computational time. The consequences of the LWT type-1 transform is passed through modified filter at σ_s = 0.5, where σ_s shows the spatial sigma which regulates the spatial weight of the bilateral filter σ_r=7 which regulates the weight of the bilateral filter. The iteration value of the modified Gaussian filter is taken as 500. The consequences of the modified Gaussian filter is pointed applying BHPF (Butterworth High Pass Filter) at a cut off volume 50 and by 7. The fusion of high frequency components is done by applying wavelet energy compaction and is provided as

$$F_1(w_t) = \sum_q^M \sum_r^N \frac{h_f(qr)}{M\times N} \qquad (7)$$

where w_t offers the neighborhood window of size $M \times N$ and $h_f(qr)$ symbolize the high-frequency wavelet coefficients at pixels coordinates (q, r). Similarly, the low-frequency coefficients of images and mask applying wavelet transform techniques is provided as:

$$F_2(w_t) = \sum_q^M \sum_r^N \frac{l_f(qr)}{M\times N} \qquad (8)$$

where w_t offers the neighborhood window of size $M \times N$ and $l_f(qr)$ shows the low-frequency wavelet coefficients at pixels coordinates (j, k).

The addition of the high frequency and low frequency components may be given as

$$F(w_t) = F_1(w_t)+ F_2(w_t) \qquad (9)$$

The high and low frequency coefficients of the fused image are reconstructed by appling inverse wavelet transform to $F(w_t)$. Both high and low volume information are contained in these re-constructed components .

IV. Experimental results

The proposed fusion algorithm is designed and implemented in MATLAB 2013a tool using image processing toolbox. The proposed technique is applied on numerous standard referenced images for which the outcomes are evaluated. Initial test is done by considering a non-naturally created image with various concentration levels.

International Journal Of Electronics Engineering (Issn: 0973-7383)
Volume 10 • Issue 2 pp. 201-209 June 2018-Dec 2018 www.csjournals.com

Figure 1: Standard images for fusion

Figure 1 shows 48 standard images which are used for empirical testing as well. Each image is pre-processed to make multi-focused by using Gaussian blur with 9 * 9 filter size and 48 * 2 = 96 pictures are obtained. Left and right sides were blurred by convolving them using averaging filter for each side. Therefore, each image acts as a referred image where as its two partially Gaussian blurred images are said to be input images for fusion process. Nevertheless, this work is not limited to these set of images only, which are considered just to have the standardized comparison with existing researches.

Figure 2: Visual analysis of felora image (a) Partially blurred image 1, (b) Partially blurred image (c) DWT, (d) BWT, (e) NSCT, and (f) Proposed technique

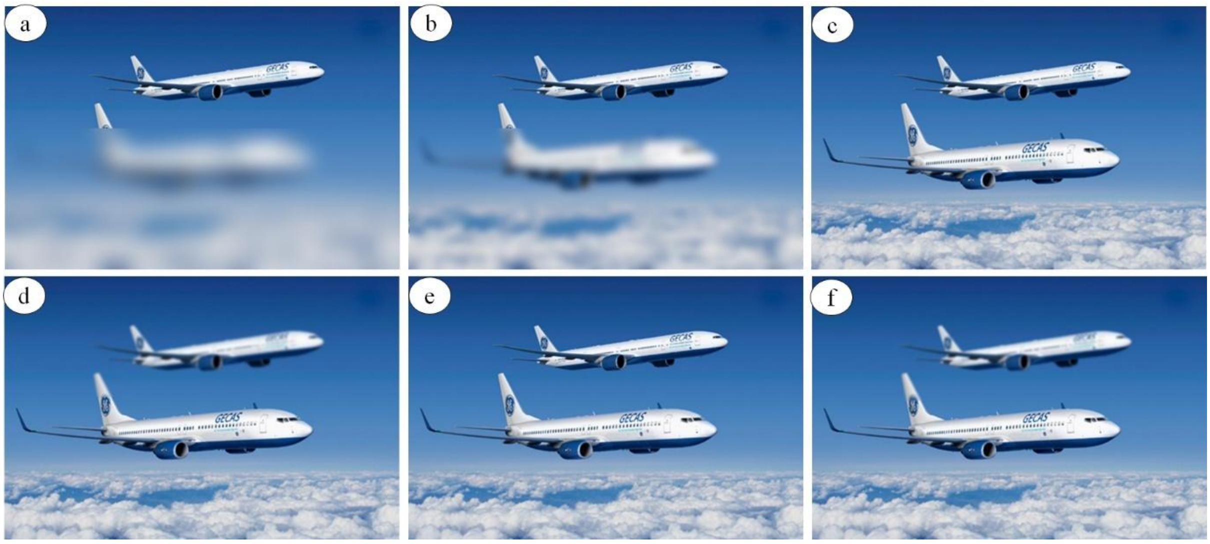

Figure 3: Visual analysis of airplane image (a) Partially blurred image 1, (b) Partially blurred image (c) DWT, (d) BWT, (e) NSCT, and (f) Proposed technique

Figure 2 and 3 shows the visual analysis of the proposed and existing competitive image fusion techniques. It is found that the proposed technique shows significantly better spatial and spectral information. Also, compared to DWT and BWT based image fusion technique it shows lesser halo and gradient reversal artifacts. Also, compared to NSCT it shows better edge preservation rate and lesser color distortion. Therefore, from visual analysis it is found that the proposed technique provides visually superior results compared to existing fusion techniques.

In addition to the visual analysis, quantitative analysis is also done. Table 1, 2, 3, 4 and 5 show the comparison of existing and the proposed image fusion techniques based upon the Mean Spatial Frequency, Mean Mutual Information, Mean Pertrovic Metric, Peak Signal to Noise Ratio and Mean Structural Similarity Index metrics. From these tables, it is clearly observed that the proposed technique provides quite significant results over existing image fusion techniques. Therefore, proposed technique shows significant improvement over the existing techniques.

Table 1: Mean spatial frequency analysis

Image	DWT	BWT	NSCT	Proposed
Felora	6.3967	6.4314	6.8530	**6.9173**
Airplane	6.8119	6.9106	6.9321	**7.0497**
Girl	6.7946	6.7818	6.7510	**6.9327**
House	6.7749	6.6738	6.8132	**6.9448**
Cameraman	6.8173	7.8455	6.9718	**7.0909**
Remote sensing	6.8687	6.9361	7.0760	**7.1893**
Cars	6.7944	6.8693	7.1399	**7.2377**
Underwater	6.7998	6.7197	6.8133	**6.9601**
Lena	6.7599	6.7499	6.8739	**7.1692**
Timepiece	6.8091	6.9150	7.0401	**7.1112**

Table 2: Mean mutual information analysis

Image	DWT	BWT	NSCT	Proposed
Felora	7.7803	7.2348	7.5470	**7.9294**
Airplane	7.3897	7.3532	7.2963	**7.9757**
Girl	7.2417	7.7212	7.7447	**7.9868**
House	7.4039	7.6154	7.7890	**7.9359**

Cameraman	7.6965	7.7430	7.7868	**7.9468**
Remote sensing	7.7320	7.6690	7.7835	**7.9103**
Cars	7.8421	7.8691	7.8785	**7.9085**
Underwater	7.8561	7.7317	7.8256	**7.9108**
Lena	7.5752	7.6477	7.7802	**7.9176**
Timepiece	7.6598	7.6509	7.6811	**7.9948**

Table 3: Mean Pertrovic metric analysis

Image	DWT	BWT	NSCT	Proposed
Felora	5.7443	6.2077	6.3119	**6.4949**
Airplane	5.8786	5.9012	5.9234	**6.0622**
Girl	6.8116	5.9709	5.9302	**6.0128**
House	5.7328	5.9305	6.1848	**6.2112**
Cameraman	5.9507	5.8443	5.9049	**6.2217**
Remote sensing	5.9390	6.1948	5.9797	**6.1174**
Cars	5.8759	6.2259	6.2389	**6.2967**
Underwater	6.5502	6.1707	6.1734	**6.2188**
Lena	5.6225	6.2277	5.9581	**6.4242**
Timepiece	5.9870	5.8357	6.1087	**6.2179**

Table 4: Peak signal to noise ratio analysis

Image	DWT	BWT	NSCT	Proposed
Felora	82.0855	83.9631	84.0377	**86.1068**
Airplane	81.2625	82.5468	83.8852	**85.6538**
Girl	82.8010	84.5211	86.9133	**87.4942**
House	83.0292	83.2316	84.7962	**86.7791**
Cameraman	83.9289	82.4889	84.0987	**87.7150**
Remote sensing	81.7303	83.6241	82.2619	**85.9037**
Cars	79.4886	81.6791	80.3354	**83.8909**
Underwater	78.5785	81.3955	83.6797	**86.3342**
Lena	76.2373	76.3674	78.1366	**79.6987**
Timepiece	77.4588	79.9880	81.7212	**81.1978**

Table 5: Mean structural similarity index metrics

Image	DWT	BWT	NSCT	Proposed
Felora	0.8305	0.8629	0.8596	**0.8996**
Airplane	0.7441	0.8399	0.8820	**0.9186**
Girl	0.7796	0.8465	0.8424	**0.8730**
House	0.8199	0.8287	0.8714	**0.9190**
Cameraman	0.7947	0.8799	0.8216	**0.8903**
Remote sensing	0.7899	0.8679	0.8967	**0.8938**
Cars	0.8177	0.8487	0.8681	**0.9124**
Underwater	0.7594	0.8327	0.8475	**0.8953**
Lena	0.7955	0.8105	0.8224	**0.8735**
Timepiece	0.7767	0.8211	0.8499	**0.8632**

V. Conclusion and Future work

Multi-focus image fusion inherits vital information from the given set of images to generate one single outcome being more informative in nature. This paper has proposed a simple and real-time mechanism by using Discrete LWT transform. Use of fusion rules has an ability to find best possible alternative in more proficient manner than other conventional advanced methods. We have described the details of algorithm design and implementation along with its visual and quantitative findings. Testing has been has carried out on a variety of images with and without consistency verification. The methodology, by means of consistency verification has empirically shown quite an effective improvement over contemporary technique. It has consistently performed well for the following state of the art metrics: Mean Spatial Frequency, Mean Mutual Information, Mean Pertrovic Metric, Peak Signal to Noise Ratio and Mean Structural Similarity Index metrics. Experimental results reveal that for propose algorithm, Mean Spatial Frequency = 8.9368, Mean Mutual Information = 7.9789, Mean Pertrovic Metric ≈ 0.95002 which are considerably superior compared to existing techniques in all cases. Moreover, it yields Peak Signal to Noise Ratio (PSNR) ≈ 99.99 % and Mean Structural Similarity Index (MSSI) ≈ 99.99 % which makes it well suitable for building highly efficient multi-focus image fusion framework.

References

[1] G. Qi, Q. Zhang, F. Zeng, J. Wang and Z. Zhu, "Multi-focus image fusion via morphological similarity-based dictionary construction and sparse representation," in CAAI Transactions on Intelligence Technology, vol. 3, no. 2, pp. 83-94, 6 2018.

[2] Y. Dongsheng, H. Shaohai, L. Shuaiqi, M. Xiaole and S. Yuchao, "Multi-focus image fusion based on block matching in 3D transform domain," in Journal of Systems Engineering and Electronics, vol. 29, no. 2, pp. 415-428, April 2018.

[3] M. Amin-Naji, P. Ranjbar-Noiey and A. Aghagolzadeh, "Multi-focus image fusion using Singular Value Decomposition in DCT domain," 2017 10th Iranian Conference on Machine Vision and Image Processing (MVIP), Isfahan, 2017, pp. 45-51.

[4] J. Wang, L. Liu, X. Zhu, N. Ai and K. Yan, "Multi-focus image fusion with online sparse dictionary learning," 2017 8th IEEE International Conference on Software Engineering and Service Science (ICSESS), Beijing, 2017, pp. 406-409.

[5] W. Zhao, D. Wang and H. Lu, "Multi-focus image fusion with a natural enhancement via joint multi-level deeply supervised convolutional neural network," in IEEE Transactions on Circuits and Systems for Video Technology.

[6] W. Li, Y. Cheng, Y. Sun and S. Xu, "Multi-focus Image Performance Evaluation Method Based on the Extraction and Combination of Multiple Metrics," 2017 13th International Conference on Computational Intelligence and Security (CIS), Hong Kong, 2017, pp. 130-134.

[7] S. Liu, J. Zhang and J. Chen, "Multi-focus image fusion using Gaussian filter and dynamic programming," 2017 Asia-Pacific Signal and Information Processing Association Annual Summit and Conference (APSIPA ASC), Kuala Lumpur, 2017, pp. 1182-1185.

[8] S. Aymaz and C. Köse, "Multi-focus image fusion using Stationary Wavelet Transform (SWT) with Principal Component Analysis (PCA)," 2017 10th International Conference on Electrical and Electronics Engineering (ELECO), Bursa, 2017, pp. 1176-1180.

[9] Y. Chen, J. Guan and W. K. Cham, "Robust Multi-Focus Image Fusion Using Edge Model and Multi-Matting," in IEEE Transactions on Image Processing, vol. 27, no. 3, pp. 1526-1541, March 2018.

[10] X. Liu and U. Kintak, "A novel multi-focus image-fusion scheme based on non-uniform rectangular partition," 2017 International Conference on Wavelet Analysis and Pattern Recognition (ICWAPR), Ningbo, 2017, pp. 53-58.

[11] X. Li, L. Wang, J. Wang and X. Zhang, "Multi-focus image fusion algorithm based on multilevel morphological component analysis and support vector machine," in IET Image Processing, vol. 11, no. 10, pp. 919-926, 10 2017.

[12] Z. Chen, D. Wang, S. Gong and F. Zhao, "Application of multi-focus image fusion in visual power patrol inspection," 2017 IEEE 2nd Advanced Information Technology, Electronic and Automation Control Conference (IAEAC), Chongqing, 2017, pp. 1688-1692.

[13] Q. Jiang, X. Jin, S. J. Lee and S. Yao, "A Novel Multi-Focus Image Fusion Method Based on Stationary Wavelet Transform and Local Features of Fuzzy Sets," in IEEE Access, vol. 5, pp. 20286-20302, 2017.

[14] James, Alex Pappachen, and Belur V. Dasarathy. "Medical image fusion: A survey of the state of the art." *Information Fusion* 19 (2014): 4-19.

[15] Haghighat, Mohammad Bagher Akbari, Ali Aghagolzadeh, and Hadi Seyedarabi. "Multi-focus image fusion for visual sensor networks in DCT domain." Computers & Electrical Engineering 37, no. 5 (2011): 789-797.
[16] Cao, Liu, Longxu Jin, Hongjiang Tao, Guoning Li, Zhuang Zhuang, and Yanfu Zhang. "Multi-focus image fusion based on spatial frequency in discrete cosine transform domain." IEEE signal processing letters 22, no. 2 (2015): 220-224.
[17] Begill, Arun, Shruti Puniani, Kamaljot Singh, and Navjot Kaur. "Evaluating the performance of max current AC-DCT based colored digital image fusion for Visual Sensor Network's." In Signal Processing and Signal Processing Education Workshop (SP/SPE), 2015 IEEE, pp. 397-402. IEEE, 2015.
[18] Mohan, Chinnem Rama, and Siddavaram Kiran. "Image Enrichment Using Single Discrete Wavelet Transform Multi-resolution and Frequency Partition." In Artificial Intelligence and Evolutionary Computations in Engineering Systems, pp. 87-98. Springer, Singapore, 2018.
[19] Cheng, Jian, Haijun Liu, Ting Liu, Feng Wang, and Hongsheng Li. "Remote sensing image fusion via wavelet transform and sparse representation." ISPRS Journal of Photogrammetry and Remote Sensing 104 (2015): 158-173.
[20] Dong, Limin, Qingxiang Yang, Haiyong Wu, Huachao Xiao, and Mingliang Xu. "High quality multi-spectral and panchromatic image fusion technologies based on Curvelet transform." Neurocomputing 159 (2015): 268-274.
[21] Wang, Shui-Hua, Tian-Ming Zhan, Yi Chen, Yin Zhang, Ming Yang, Hui-Min Lu, Hai-Nan Wang, Bin Liu, and Preetha Phillips. "Multiple sclerosis detection based on biorthogonal wavelet transform, RBF kernel principal component analysis, and logistic regression." IEEE Access 4 (2016): 7567-7576.
[22] Thomas, Elizabeth, Praseeda B. Nair, Sherin N. John, and Merry Dominic. "Image fusion using daubechies complex wavelet transform and lifting wavelet transform: A multiresolution approach." In Emerging Research Areas: Magnetics, Machines and Drives (AICERA/iCMMD), 2014 Annual International Conference on, pp. 1-5. IEEE, 2014.
[23] Zhang, Yongxin, Li Chen, Zhihua Zhao, Jian Jia, and Jie Liu. "Multi-focus image fusion based on robust principal component analysis and pulse-coupled neural network." Optik-International Journal for Light and Electron Optics 125, no. 17 (2014): 5002-5006.
[24] Nandi, Dibyadeep, Amira S. Ashour, Sourav Samanta, Sayan Chakraborty, Mohammed AM Salem, and Nilanjan Dey. "Principal component analysis in medical image processing: a study." International Journal of Image Mining 1, no. 1 (2015): 65-86.
[25] Shahdoosti, Hamid Reza, and Hassan Ghassemian. "Combining the spectral PCA and spatial PCA fusion methods by an optimal filter." Information Fusion 27 (2016): 150-160.
[26] Palsson, Frosti, Johannes R. Sveinsson, Magnus Orn Ulfarsson, and Jon Atli Benediktsson. "Model-based fusion of multi-and hyperspectral images using PCA and wavelets." IEEE transactions on Geoscience and Remote Sensing 53, no. 5 (2015): 2652-2663.
[27] Lee, Geun-Young, Sung-Hak Lee, and Hyuk-Ju Kwon. "DCT-Based HDR Exposure Fusion Using Multiexposed Image Sensors." Journal of Sensors 2017 (2017).
[28] Ahmad, Muhammad Imran, Nurain Mohamad, Mohd Nazrin Md Isa, Ruzelita Ngadiran, and Abdul Majid Darsono. "Fusion of Low Frequency Coefficients of DCT Transform Image for Face and Palmprint Multimodal Biometrics." In Cybernetics (CYBCONF), 2017 3rd IEEE International Conference on, pp. 1-5. IEEE, 2017.
[29] Li, Shutao, Xudong Kang, and Jianwen Hu. "Image fusion with guided filtering." IEEE Transactions on Image Processing 22, no. 7 (2013): 2864-2875.
[30] Yadav, Satya Prakash, and Sachin Yadav. "Fusion of Medical Images in Wavelet Domain: A Discrete Mathematical Model." Journal of Engineering and Education 14 (2018).
[31] Zhang, Qiang, Yi Liu, Rick S. Blum, Jungong Han, and Dacheng Tao. "Sparse representation based multi-sensor image fusion for multi-focus and multi-modality images: a review." Information Fusion 40 (2018): 57-75.
[32] Ferraris, Vinicius, Nicolas Dobigeon, Qi Wei, and Marie Chabert. "Detecting changes between optical images of different spatial and spectral resolutions: a fusion-based approach." IEEE Transactions on Geoscience and Remote Sensing 56, no. 3 (2018): 1566-1578.
[33] Darwish, Saad M. "Multi-level fuzzy contourlet-based image fusion for medical applications." IET image processing 7, no. 7 (2013): 694-700.